

# A GEM-based Optically Readout Time Projection Chamber for charged particle tracking

V. C. Antochi,<sup>1, a)</sup> G. Cavoto,<sup>1, b)</sup> I. A. Costa,<sup>1, c)</sup> E. Di Marco,<sup>1</sup> G. D'Imperio,<sup>1</sup> F. Iacoangeli,<sup>1</sup> M. Marafini,<sup>1, d)</sup> A. Messina,<sup>1, b)</sup> D. Pinci,<sup>1</sup> F. Renga,<sup>1</sup> C. Vena,<sup>1</sup> E. Baracchini,<sup>2</sup> A. Cortez,<sup>2</sup> G. Dho,<sup>2, e)</sup> L. Benussi,<sup>3</sup> S. Bianco,<sup>3</sup> C. Capoccia,<sup>3</sup> M. Caponero,<sup>3, f)</sup> G. Maccarrone,<sup>3</sup> G. Mazzitelli,<sup>3</sup> A. Orlandi,<sup>3</sup> E. Paoletti,<sup>3</sup> L. Passamonti,<sup>3</sup> D. Piccolo,<sup>3</sup> D Pierluigi,<sup>3</sup> F. Rosatelli,<sup>3</sup> A. Russo,<sup>3</sup> G. Saviano,<sup>3, g)</sup> S Tomassini,<sup>3</sup> R. A. Nóbrega,<sup>4</sup> and F Petrucci<sup>5, h)</sup>

<sup>1)</sup>Istituto Nazionale di Fisica Nucleare Sezione di Roma, I-00185, Italy

<sup>2)</sup>Gran Sasso Science Institute L'Aquila, I-67100, Italy

<sup>3)</sup>Istituto Nazionale di Fisica Nucleare Laboratori Nazionali di Frascati, I-00040, Italy

<sup>4)</sup>Universidade Federal de Juiz de Fora, Juiz de Fora, MG, 36000-000, Brazil

<sup>5)</sup>Dipartimento di Matematica e Fisica, Università Roma TRE, Roma, I-00146, Italy

(Dated: 17 June 2020)

The Time Projection Chamber (TPC) is an ideal candidate to track particles in a wide range of energies. Large volumes TPCs can be readout with a suitable number of channels offering a complete 3D reconstruction of the charged particle tracks and of their released energy allowing the identification of their mass. Moreover, He-based TPC's are very promising to study keV energy particles, opening the possibility for directional searches of Dark Matter (DM) and the study of Solar Neutrinos (SN). On the other hand, in order to reach a keV energy threshold, a large number of channels is required to obtain a high granularity, that could be expensive and hard to manage.

A small prototype (named LEMOn) to test and validate an innovative read-out technique is described here. It based on the amplification of the ionization in Micro Pattern Gas Detector (MPGD) producing visible light collected by a sub-millimeter position resolution sCMOS (scientific CMOS) camera. This type of readout - in conjunction with a fast light detection - allows a 3D reconstruction of the tracks, a sensitivity to the track direction and a very promising particle identification capability useful to distinguish DM nuclear recoils from a  $\gamma$ -induced background.

**Large Time Projection Chambers (TPC) have various applications in high energy physics and nuclear physics. These detectors are among the best in offering good charged particle energy resolution and to allow the identification of the particle's mass. This can be obtained along with a very good performance in tracking the particle's trajectory with competitive spatial resolution. The study of such a technology for ultra-rare events searches as the directional search of Dark Matter<sup>1-3</sup> (DM) and the detection of neutrinos coming from the Sun (SN)<sup>4,5</sup> is currently being pursued by several groups, which are part of the CYGNUS<sup>6</sup> international network<sup>7</sup>.**

**A longer term project for tens of  $m^3$  volume TPC requires the construction of  $1\ m^3$  demonstrators. In this paper we describe the performance of a smaller 7 litres prototype (named LEMOn) in tracking ultra-relativistic electrons. LEMOn is based on Micro Pattern Gaseous Detectors (MPGD), namely a large triple Gas Electron Multiplier (GEM)<sup>8</sup>, optically read-out by means of a low noise and high granularity sCMOS sensor<sup>9,10</sup>.**

Many smaller scale prototypes have been tested so far showing promising results to design the CYGNO  $1\ m^3$  demonstrator to be constructed in 2020-2021 and to be hosted at the INFN National Laboratory of Gran Sasso (LNGS). In a later phase, a  $30-100\ m^3$  detector is foreseen, as a brick of a world distributed observatory for DM and SN within the CYGNUS international network.

## I. INTRODUCTION

The purpose of the current R&D phase is to asses the performance of a relatively large TPC based on the drift of the ionization electrons within a He-based gas mixture operated at atmospheric pressure and equipped with a high granularity and high sensitivity optical readout of GEMs. In this respect the test of the LEMOn prototype with ultra-relativistic electrons presented here is meant to study the capability of the optically readout TPC to detect and to reconstruct within the TPC drift region the positions of clusters with few ionization electrons each. The pattern of contiguous clusters represents the "track" of the ultra-relativistic electron trajectory and are exploited to identify it, demonstrating that LEMOn would also be an excellent beam monitoring device.

In absence of a reference time for the events, electron drift time can not be exploited to extract information about their depth inside the detector. In this paper, we study a method to measure the longitudinal position of an ionizing particle in the TPC drift volume based on the electron diffusion and there-

<sup>a)</sup>Also at Dipartimento di Fisica Sapienza Università di Roma, I-00185, Italy now at Oskar Klein Centre, Department of Physics, Stockholm University, AlbaNova, Stockholm SE-10691, Sweden

<sup>b)</sup>Also at Dipartimento di Fisica Sapienza Università di Roma, I-00185, Italy

<sup>c)</sup>Also at Universidade Federal de Juiz de Fora, Juiz de Fora, MG, Brazil

<sup>d)</sup>Also at Museo Storico della Fisica e Centro Studi e Ricerche "Enrico Fermi" Piazza del Viminale 1, Roma, I-00184, Italy

<sup>e)</sup>Also at Istituto Nazionale di Fisica Nucleare, Laboratori Nazionali del Gran Sasso, Assergi, I-67100, Italy

<sup>f)</sup>Also at ENEA Centro Ricerche Frascati, Frascati, I-00044, Italy

<sup>g)</sup>Also at Dipartimento di Ingegneria Chimica, Materiali e Ambiente, Sapienza Università di Roma, Roma, I-00185, Italy

<sup>h)</sup>Also at Istituto Nazionale di Fisica Nucleare, Sezione di Roma TRE, Roma, I-00146, Italy

fore without relying on the time of the particle interaction in the gas which is unknown in DM search. It helps to fully define a fiducial gas volume, so that background events generated by the detector components, in particular the cathode and the amplification system (as the GEMs), can be discarded.

The MPGD optical readout can in fact represent a change in the paradigm of TPCs for rare events searches:

- optical sensors offer higher granularity with respect to electron sensitive devices;
- optical coupling allows to keep the sensors out of the sensitive volume, reducing the interference with the high voltage operation and the gas contamination;
- the use of suitable lenses enables the imaging of large surfaces to small sensors.

Moreover, in last years, optical sensors market had an impressive development: sensors able to provide the required large granularity along with a very low noise level and high sensitivity to single photon counting are now available.

Recently, many tests have been conducted with different prototypes (NITEC<sup>11</sup>, ORANGE<sup>12,13</sup>, LEMON<sup>14-16</sup>) with various particles sources (electron beam test facility, neutron beams and different radioactive sources). In the following, we report the results obtained with the LEMOn prototype at the Frascati Beam Test Facility (BTF).

## II. LEMON PROTOTYPE DESIGN

The LEMOn prototype structure (Fig. 2) was made of ASA, Acrylonitrile Styrene Acrylate, at the 3D printing Facility of the National Laboratory of Frascati (LNF)<sup>17</sup> of INFN. This has offered the opportunity to easily design and to quickly develop detectors and also to test the 3D printing system for gas detector applications.

The LEMOn's heart consists of a 7 liter active drift volume surrounded by a  $200 \times 240 \text{ mm}^2$  elliptical field cage with a 200 mm distance between the anode and the cathode. The electric field is shaped by 1 mm Cu+Ag wires held at their positions by nineteen 3D-printed rings. The anode side is instrumented with a  $200 \times 240 \text{ mm}^2$  rectangular triple GEM structure located at a position 10 mm apart from the last field cage ring. They are LHCb-like<sup>18</sup> GEMs with 70  $\mu\text{m}$  diameter holes and 140  $\mu\text{m}$  pitch and with two 2 mm wide transfer field gaps among them (Fig. 1). A  $203 \times 254 \times 1 \text{ mm}^3$  transparent window and a bellow with a tunable length allow to collect the light emitted from the GEMs by using an ORCA-Flash 4.0 camera<sup>19</sup>. This camera is positioned at a 52 cm distance from the outemost GEM layer and is based on a sCMOS sensor with a high granularity ( $2048 \times 2048$  pixels), very low noise (around two photons per pixel), high sensitivity (70% quantum efficiency at 600 nm) and good linearity. This camera is instrumented with a Schneider lens ( $f/0.95-25 \text{ mm}$ ). The lens is placed at a distance  $d$  of 50.6 cm from the last GEM in order to obtain a de-magnification  $\delta = (d/f) - 1 = 19.25$  to image a surface  $25.6 \times 25.6 \text{ cm}^2$  onto the  $1.33 \times 1.33 \text{ cm}^2$  sensor. In this configuration, each pixel is therefore imaging an effective

area of  $125 \times 125 \mu\text{m}^2$  of the GEM layer. The fraction of the light collected by the lens can be evaluated<sup>9</sup> to be  $1.7 \times 10^{-4}$ .

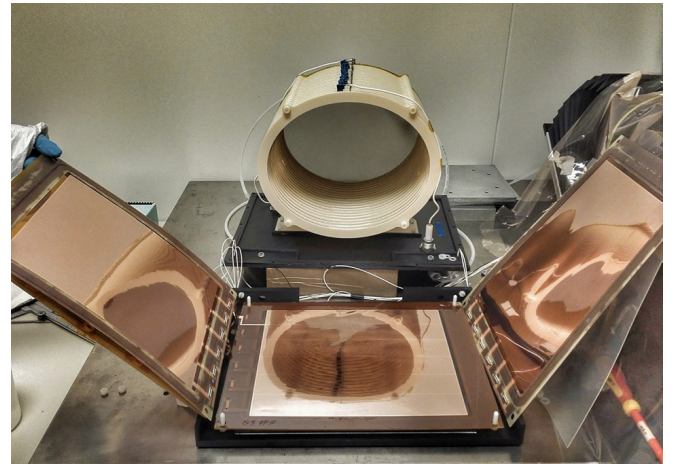


FIG. 1. Exploded triple GEM structure (on the front) with the 3D-printed field cage rings (white) equipped with a semi-transparency cathode (on the back of the rings).

On the cathode side, LEMOn has been equipped with a  $50 \times 50 \text{ mm}^2$  HZC Photonics XP3392 photomultiplier<sup>20</sup> (PMT) detecting light through a transparent  $50 \times 50 \times 4 \text{ mm}^3$  fused silica window.

This PMT also allowed to study - mainly for timing purpose - the primary scintillation light emitted in the drift volume by the BTF electrons themselves and the secondary light produced by the innermost GEM layer 200 mm far away during the development of the electron avalanche. A cathode has been realized using an ATLAS MicroMegas mesh, produced by Swiss BOOP company, stretched and glued on ring, 1 cm apart from the last ring of the field cage and ensuring an adequate light transmission. Its transparency to light has been estimated to be about 70%. The field cage is contained in a  $370 \times 270 \times 280 \text{ mm}^3$  and 2.5 mm thick box. This box has been equipped with two 180  $\mu\text{m}$  thin  $200 \times 200 \text{ mm}^2$  windows made of TEDLAR in order to guarantee the gas containment and to reduce as much as possible the multiple scattering of the impinging ultra-relativistic electrons (or the absorption of other particles).

## III. DETECTOR OPERATIONS

The data reported in this paper have been collected at the Frascati Beam Test Facility<sup>21</sup> which can deliver bunched electrons or positrons from few tens of MeV to several hundred MeV energy. The BTF is optimized to deliver electrons with an energy of 450 MeV with a typical beam spot size of  $\sigma_{x,y} \simeq 2 \text{ mm}$ , a divergence  $\sigma'_{x,y} \simeq 2 \text{ mrad}$ , and an energy spread of  $\simeq 1\%$ . Moreover, for our measurements the bunch multiplicity has been tuned to be single particle, with the possibility to change it up to several hundred electrons (with 10 ns bunch length). The bunch multiplicity and the beam spot-size were monitored by means of a Fitpix<sup>22</sup> detector located up-

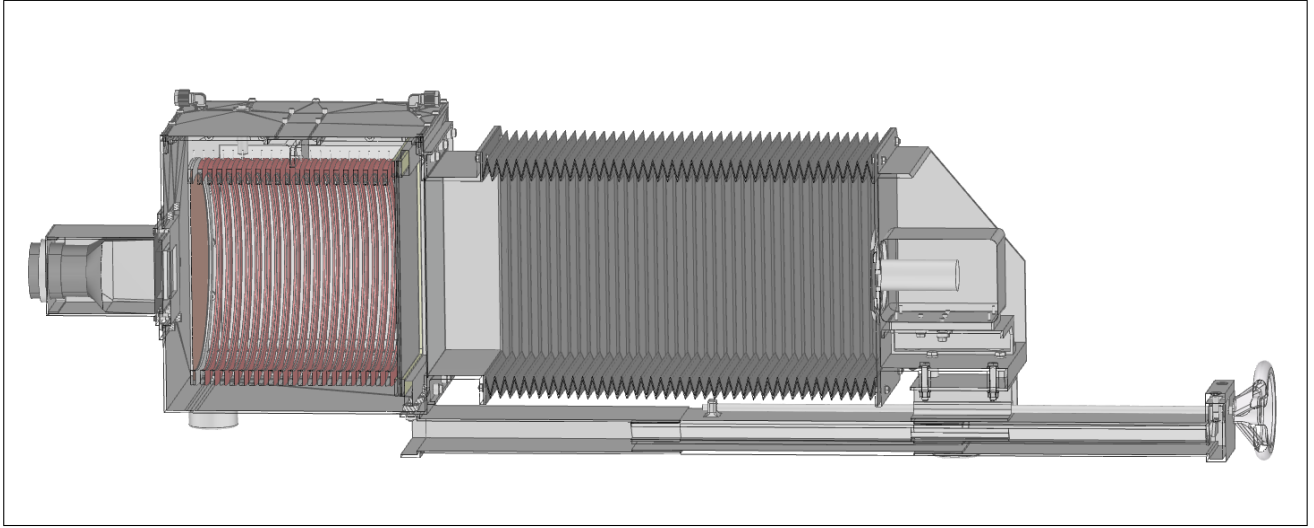


FIG. 2. LEMOn 3D printing design. From the left to the right: PMT holder, semi-transparent cathode, field cage rings (in red), the triple GEM stack,a large transparent window, the optical bellow and the ORCA Flash camera holder.

stream of LEMOn and a Pb-glass calorimeter<sup>23 24</sup> accommodated at the back of LEMOn and acquired in coincidence with the LEMOn camera image and the PMT signal.

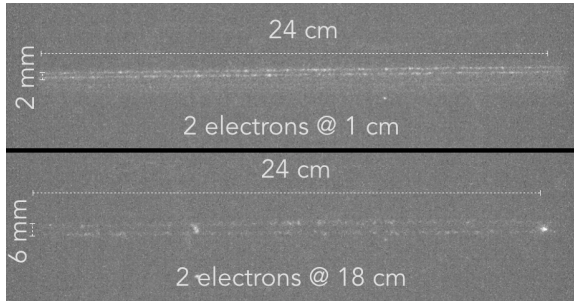


FIG. 3. Two examples of two-tracks events collected at the Frascati BTF. The two BTF electrons are crossing the field cage parallel to the 240 mm major axis. One event is acquired with the beam close to the GEM (up), and another with the beam 180 mm far away from the GEM (down). The separation among the two track can be easily measured.

LEMON was operated at BTF with a He-CF<sub>4</sub> (60/40) gas mixture, the triple GEM system set at a voltage across the GEM sides of 455 V and an electric field between them of 2.0 kV/cm. The gas mixture was kept at atmospheric pressure under continuous flow of about 100 cc/min and with the GEMs operated at very high gain ( $> 5 \times 10^5$ ) in order to reach a good light production in the avalanche generated in the GEMs structure. The typical photon yield for this type of gas mixtures has been measured to be around 0.07 photons per avalanche electron.<sup>9,25,26</sup>

The field cage was powered by a CAEN N1570.<sup>27</sup> This posed a limitation to the maximum electric field at 0.6 kV/cm.

Some data has also been collected at a lower field in order to study the field cage performance. The triple GEM system was powered with a HV GEM power supply<sup>28</sup> ensuring stability

and accurate monitoring of the bias currents.

The ORCA Camera I/O has been configured in order to get a pre-trigger, that must occur 80  $\mu$ s before the shutter, and to synchronize the PMT signal waveform acquired with an oscilloscope LeCroy 610Zi. Optics and exposure time (30 ms) were optimized to ensure the largest light collection and to avoid events due to the natural radioactivity. Between 100 and 300 images were typically acquired per run. Fig. 3 shows two examples of BTF electron tracks images acquired with LEMOn.

The 450 MeV BTF electrons were delivered by the LNF accelerator complex along the X axis direction (see Fig.4) with a repetition rate of one bunch every second. LEMOn was accommodated over a remotely controlled table in order to scan the Y and Z coordinates (with a 0.2 mm precision).

#### IV. TEST BEAM RESULTS

Data were collected at the LNF BTF during a week long campaign, when LEMOn was continuously operated.

The fast PMT signal waveform was acquired using as external trigger from the timing signal of the BTF line synchronized with the electrons arrivals. The time  $t_s$  corresponding to a fixed voltage of the PMT waveform was associated to each PMT signal and data at different longitudinal Z position were collected. The standard deviation ( $SD_t$ ) of the distribution of the residuals of  $t_s$  at each Z can be converted into the standard deviation ( $SD_Z$ ) of the BTF electrons Z position using the gas mixture drift velocity. A value of  $SD_Z$  around 1 mm was found, well compatible with the beam spot transverse size.

Each image acquired with the sCMOS camera was saved as a 2048 x 2048 matrix of photon counts. Because of the very low occupancy of sensor, the baseline noise of the sensor is estimated pixel by pixel by obtaining the distribution of counts for each pixel in all the images of a data-taking run. The av-

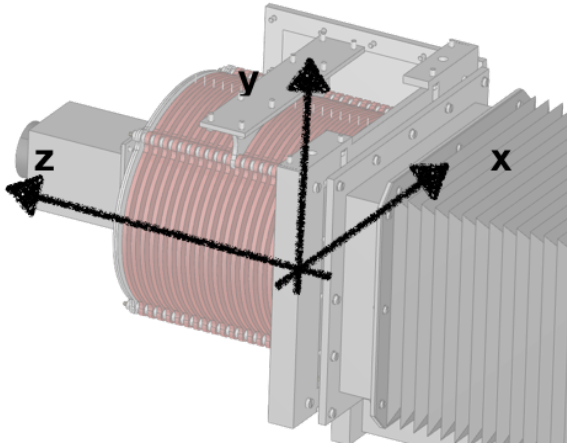


FIG. 4. Reference frame: the origin of the axis is located at the middle of the GEM plane in vertical Y coordinate, while the X origin is located at the beginning of the GEM plane to coincide with the particle track length; moreover, the Z coordinate represents the distance from the GEM plane starting from it

erage count and the standard deviation ( $\sigma_n$ ) for each pixel is then evaluated. This average photon count is subtracted to the count of each image before the image is further processed.

The reconstruction of tracks in each image is then made by using a Hough transform pattern recognition algorithm (HT)<sup>29</sup>. Since LEMOn is positioned to let the BTF electrons cross the drift volume at  $Y \sim 0$ , only pixels with a photon count exceeding  $1.5\sigma_n$  are used in the HT. The HT could finds several lines connecting all the pixels above this threshold: the most ranked line within an angle of about  $\pm 5$  mrad respect to the X axis is then selected in each image and it represents the candidate reconstructed BTF electron (a *track*). Multiple track images are also analyzed and the HT is in fact able to distinguish tracks in events with multiplicity larger than one.

The efficiency to reconstruct a BTF electron crossing the 24 cm wide drift region it is measured to be very close to unit. In fact, a Garfield<sup>30,31</sup> simulation of the gas mixture yields an estimate for the average energy loss of 0.20 keV/mm for a  $\simeq 450$  MeV electron. This energy loss translates into three primary ionization  $e^-$  cluster per mm. The sequence of several ionization clusters along the BTF electron trajectory is in fact a clear signature to detect each BTF electron. We check this prediction by selecting in the runs the events with a Pb-glass calorimeter signal compatible with a single BTF electron deposit. In these events we always find a BTF track in the sCMOS image.

#### A. Tracking performances

The total light yield distribution transverse to the track direction is obtained for each track (Fig. 5). This distribution is fitted to a Gaussian function and its integral is proportional to the total energy loss of the track in the gas volume of the field cage.

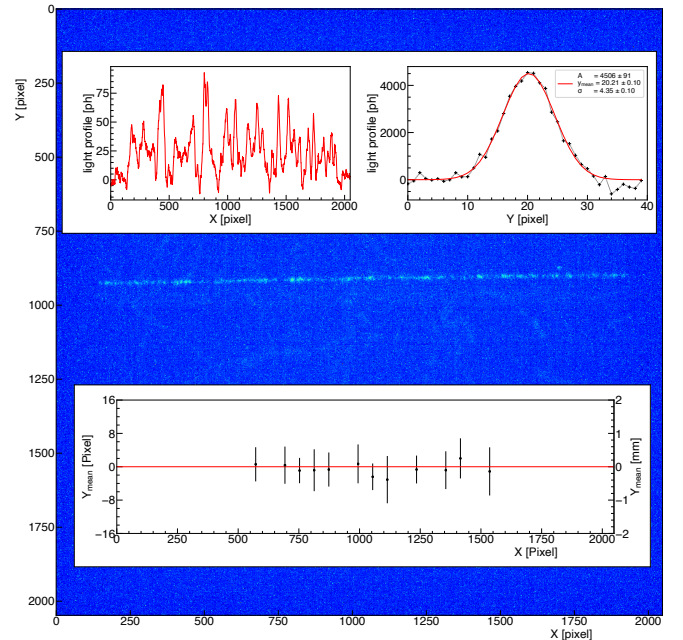


FIG. 5. **Background:** sCMOS camera image collected at the LNF BTF 6.5 cm apart from GEM plane, pixels with a number of counts larger than the average noise and due to a BTF electron are visible at  $Y \sim 1000$ . **Left top insert:** light distribution (after pixel-by-pixel noise subtraction) along the track X-direction summing all the photons for 40 pixel in the Y direction around the track direction. **Right top insert:** light distribution transverse to the track (Y direction) summing all the photons along the X direction with a superimposed Gaussian fit. **Bottom insert:** Gaussian  $Y_{mean}$  of the transverse light distribution for each of the 18 segments with the line found by the HT. The error bar of the points is the sigma of the normal fit in each slice and it is taken as a indication of the width of the light deposit. Some segments with a too low signal-to-noise ratio of the detected light are not displayed.

In different runs the LEMOn position along Z is changed resulting in a different Z coordinate for the tracks. These runs are used to evaluate the uniformity of the response across the field cage. The total light yield per track is in fact fairly uniform, with a slight decrease at Z positions farther away from the GEMs (see Fig.6). This is likely due to the electron attachment to gas impurities during the drift of the ionization electrons from their production points along the track to the GEMs. Moreover, the relative fluctuation of the total light yield per track represents an estimate of the energy loss resolution of LEMOn (Fig.7). This turns out to be about 20% and almost independent on the Z position of the track.

The tracks can be divided in 36 portions of about 7 mm long - which are segments belonging to the same track. We evaluate the performance of LEMOn in measuring their position in space. An average energy loss of about 1.5 keV corresponds to each segment: this allows to study the performance of LEMOn to tiny energy release and - in perspective - to predict a very small energy threshold for the DM detection application.

Among these 36 segments only 18 segments are retained

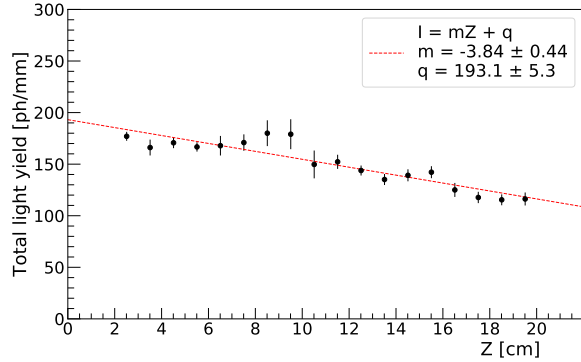


FIG. 6. Average total light yield  $I$  per track as a function of the track  $Z$  position across the field cage.

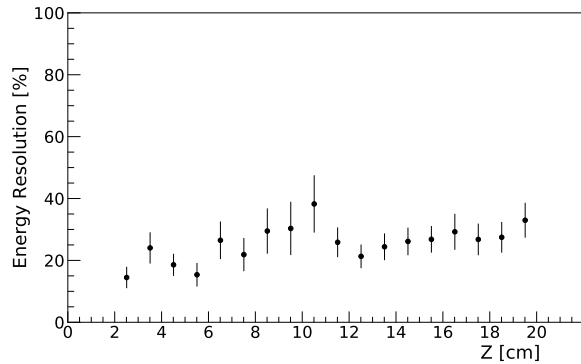


FIG. 7. Energy Resolution: standard deviation of total light yield per track divided by its average as a function of the track  $Z$  position.

in the central region of the field cage ellipse. This is due to the circumstance that an electric field distortion has been observed in regions close to the field cage rings, because of their different shape with respect to the GEM, in other LEMOn data<sup>32</sup>.

Also the transverse light profile of each segment can be described by a Gaussian distribution. The fitted mean value  $Y_{mean}$  of this distribution is used to identify the segment's  $Y$  position. In Fig. 5 examples of longitudinal and transverse light profiles are shown. The residual distribution of the 18 segments  $Y_{mean}$  with respect to line obtained with HT is then obtained. The standard deviation of this distribution evaluated in a sample of several tracks represents an estimate of the resolution on the segment's  $Y$  position. This procedure is repeated for several images acquired with the BTF electrons crossing the LEMOn field cage at different  $Z$  positions (Fig. 8). The dependence of the segment's  $Y$  position resolution on the  $Z$  track coordinate is then interpolated with a linear function (Fig.8). While the best (extrapolated) resolution of  $83 \pm 12 \mu\text{m}$  is obtained close to the GEMs ( $Z = 0$ ), we observe its worsening for larger  $Z$ : this is mainly due to the reduction of electrons for larger  $Z$  that, besides reducing the produced light, also amplifies the effect of diffusion.

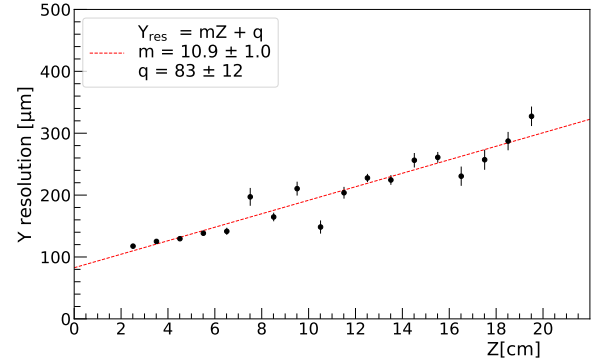


FIG. 8. Segment  $Y$  position resolution as a function of the track's  $Z$  coordinate.

## B. $Z$ coordinate measurement

While the ionization electrons are drifting in the gas, they are subject to a longitudinal and transverse diffusion. Their arrival  $X$  and  $Y$  coordinates and their arrival time at the GEMs are correlated with their production point position. The standard deviations of the position at the anode,  $\sigma_X$  and  $\sigma_Y$  are equal to  $\sqrt{\frac{2DZ}{\mu E}}$  where  $D$  is the diffusion coefficient,  $\mu$  the electron mobility and  $E$  the drift electric field<sup>33</sup>. Moreover, during the avalanche formation within the GEMs a further diffusion of the avalanche electrons is taking place. Eventually, the light recorded from the sCMOS camera and PMT is related to the original point and time with an uncertainty that is larger for production points farther in  $Z$  from the GEMs. This is reflected in the transverse ( $Y$ ) light distribution of each segment of the track: the  $\sigma_Y$  obtained from the Gaussian fit is in fact increasing with  $\sqrt{Z}$ . Therefore, the segment's original  $Z$  can be deduced by measuring  $\sigma$  (Fig.9).

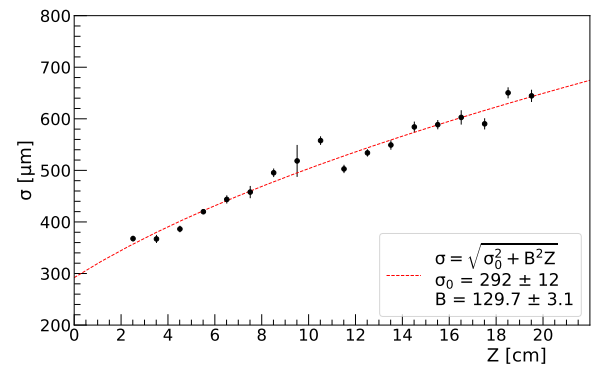


FIG. 9. Average  $\sigma$  of transverse light distribution for track segments as a function of the track  $Z$  coordinate.

The observed values of  $\sigma$  are related to the track's  $Z$  by  $\sigma = \sqrt{\sigma_0^2 + B^2 Z}$

The transverse diffusion coefficient  $B$  in the gas is measured to be  $129.7 \pm 3.1 \frac{\mu\text{m}}{\sqrt{\text{cm}}}$ , well in agreement with the expected

value obtained with Garfield simulation ( $130 \frac{\mu\text{m}}{\sqrt{\text{cm}}}$ ).

The intercept at zero  $\sigma_0 = 292 \pm 12 \mu\text{m}$  is due to the contribution of the electron avalanche propagation in the GEM stack, and it is also well in agreement with simulations.

From the same Gaussian fit to the light  $Y$  distribution of each segment, the amplitude  $A$  can be obtained. Since  $\sigma A$  is proportional to the total light  $I$  of the segment we can define  $\eta = \frac{\sigma}{A}$  that is therefore proportional to  $\frac{\sigma_0^2 + B^2 Z}{I}$ .

In Fig. 10 we show the dependence of  $\eta$  on the track's  $Z$  coordinate. A quadratic fit gives a better representation of the data. This can be understood since in our data the light  $I$  shows a linear decrease with  $Z$  (see Fig.6).

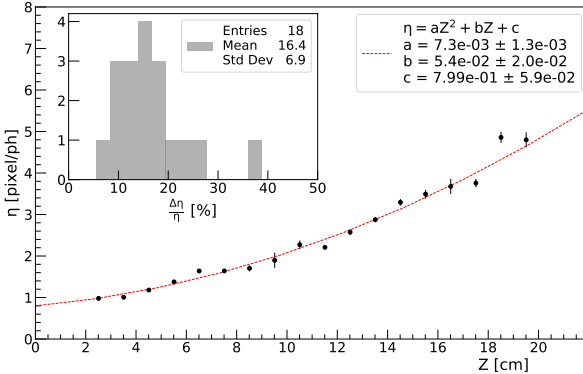


FIG. 10. Average  $\eta$  as a function of the track's  $Z$  coordinate with a quadratic fit superimposed. Relative uncertainty on  $\eta$  (inset) for the various  $Z$  positions.

A similar parameter  $\eta_{PMT}$  can be defined from the analysis of the PMT waveform. In this case the total light of the track is recorded and we use the Pb-glass calorimeter signal of the BTF line to reject events with more than one track. The amplitude of the PMT waveform and its width can be similarly used to calculate  $\eta_{PMT}$ . In this case the width of the waveform is larger for more distant tracks (larger  $Z$ ) due to the longitudinal diffusion of the drifting ionization electrons. By using the drift velocity,  $\eta_{PMT}$  can be related to  $Z$  similarly to  $\eta$  (Fig.11).

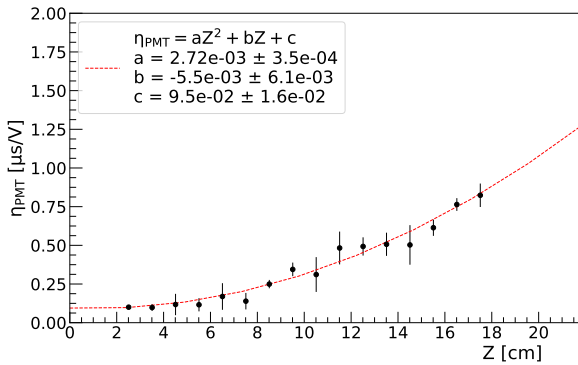


FIG. 11. Average  $\eta_{PMT}$  as a function of the track  $Z$  coordinate. Data were not recorded for the largest  $Z$  point since the beam was adding extra noise in the PMT.

Transverse and longitudinal diffusion can therefore be exploited to measure the longitudinal  $Z$  coordinates. We can estimate  $\frac{\Delta\eta}{\eta}$  from the standard deviation of the distributions of the  $\eta$  values. Since  $\frac{\Delta\eta}{\eta} = \frac{\Delta Z}{Z}$  an estimate for  $\frac{\Delta Z}{Z}$  turns to be in the range 10% - 20%.

Therefore, a combination of the  $\eta$  parameters would be very useful to define a fiducial region of a DM detector. Anode where the GEMs are located (at  $Z \sim 0$  in LEMOn) and cathode (at  $Z \sim 20$  cm in LEMOn) are usually the most radioactive elements in a DM detector. They are in fact sources of spurious nuclear recoils that would be easily removed if their  $Z$  coordinate is measured.

## V. CONCLUSION

The data collected at the Frascati Beam Test Facility with the LEMOn prototype, part of the CYGNO project, are confirming the potentiality of large optically readout TPC as detector for rare and low energy events.

In this paper we have reported how ultra-relativistic electron tracks can be very efficiently reconstructed by collecting the light emitted from GEMs with a high resolution and high sensitivity sCMOS camera and a PMT. The analysis of the 7 mm long segment of an electron track shows a good spatial and energy resolution, making very promising the use of this gas TPC down to few keV energy releases. Also a method based on the ionization electron diffusion can be very effective in determining the segment's longitudinal position within the field cage. This technology looks therefore extremely interesting in the development of a larger scale detector aiming to observe very rare processes as DM or Solar Neutrinos.

## ACKNOWLEDGMENT

A special thanks goes to M. Iannarelli, now retired, who assembled LEMOn and we are grateful to the BTF staff for the excellent and stable beam condition and their inexhaustible support.

This work was partially supported by the European Research Council (ERC) under the European Union's Horizon 2020 research and innovation program (grant agreement No 818744).

Data available on request from the authors.

- <sup>1</sup>J. Battat *et al.* (DRIFT), “Low Threshold Results and Limits from the DRIFT Directional Dark Matter Detector,” *Astropart. Phys.* **91**, 65–74 (2017), arXiv:1701.00171 [astro-ph.IM].
- <sup>2</sup>J. Battat *et al.*, “Readout technologies for directional WIMP Dark Matter detection,” *Phys. Rept.* **662**, 1–46 (2016), arXiv:1610.02396 [physics.ins-det].
- <sup>3</sup>J. Battat *et al.* (DRIFT), “First background-free limit from a directional dark matter experiment: results from a fully fiducialised DRIFT detector,” *Phys. Dark Univ.* **9–10**, 1–7 (2015), arXiv:1410.7821 [hep-ex].
- <sup>4</sup>J. Seguinot, T. Ypsilantis, and A. Zichichi, “A High rate solar neutrino detector with energy determination,” *Conf. Proc. C* **920310**, 289–313 (1992).
- <sup>5</sup>C. Arpesella, C. Broggini, and C. Cattadore, “A possible gas for solar neutrino spectroscopy,” *Astroparticle Physics* **4**, 333 – 341 (1996).

<sup>6</sup><https://web.infn.it/cygnus/>.

- <sup>7</sup>E. Baracchini, R. Bedogni, F. Bellini, L. Benussi, S. Bianco, L. Bignell, M. Caponero, G. Cavoto, E. D. Marco, C. Eldridge, A. Ezeribe, R. Gargana, T. Gamble, R. Gregorio, G. Lane, D. Loomba, W. Lynch, G. Maccarrone, M. Marafini, G. Mazzitelli, A. Messina, A. Mills, K. Miuchi, F. Petrucci, D. Piccolo, D. Pinci, N. Phan, F. Renga, G. Saviano, N. Spooner, T. Thorpe, S. Tomassini, and S. Vahsen, “Cygno: a cygnus collaboration 1 m<sup>3</sup> module with optical readout for directional dark matter search,” (2019), arXiv:1901.04190 [physics.ins-det].
- <sup>8</sup>F. Sauli, “GEM: A new concept for electron amplification in gas detectors,” Nucl. Instrum. Meth. A **386**, 531–534 (1997).
- <sup>9</sup>M. Marafini, V. Patera, D. Pinci, A. Sarti, A. Sciubba, and E. Spiriti, “High granularity tracker based on a Triple-GEM optically read by a CMOS-based camera,” JINST **10**, P12010 (2015), arXiv:1508.07143 [physics.ins-det].
- <sup>10</sup>M. Marafini, V. Patera, D. Pinci, A. Sarti, A. Sciubba, Torchia, and E. Spiriti, “Optical readout of a triple-GEM detector by means of a CMOS sensor,” Proceedings, 13th Pisa Meeting on Advanced Detectors : Frontier Detectors for Frontier Physics (FDFP 2015): La Biodola, Isola d’Elba, Italy, May 24–30, 2015, Nucl. Instrum. Meth. **A824**, 562–564 (2016).
- <sup>11</sup>E. Baracchini, G. Cavoto, G. Mazzitelli, F. Murtas, F. Renga, and S. Tomassini, “Negative ion time projection chamber operation with SF6at nearly atmospheric pressure,” Journal of Instrumentation **13**, P04022–P04022 (2018).
- <sup>12</sup>M. Marafini, V. Patera, D. Pinci, A. Sarti, A. Sciubba, and E. Spiriti, “ORANGE: A high sensitivity particle tracker based on optically read out GEM,” Proceedings, 14th Vienna Conference on Instrumentation (VCI 2016): Vienna, Austria, February 15–19, 2016, Nucl. Instrum. Meth. **A845**, 285–288 (2017).
- <sup>13</sup>V. C. Antochi, E. Baracchini, G. Cavoto, E. D. Marco, M. Marafini, G. Mazzitelli, D. Pinci, F. Renga, S. Tomassini, and C. Voena, “Combined readout of a triple-GEM detector,” JINST **13**, P05001 (2018), arXiv:1803.06860 [physics.ins-det] CITATION = ARXIV:1803.06860; .
- <sup>14</sup>D. Pinci, E. Di Marco, F. Renga, C. Voena, E. Baracchini, G. Mazzitelli, A. Tomassini, G. Cavoto, V. C. Antochi, and M. Marafini, “Cygnus: development of a high resolution TPC for rare events,” Proceedings, 2017 European Physical Society Conference on High Energy Physics (EPS-HEP 2017): Venice, Italy, July 5–12, 2017, PoS **EPS-HEP2017**, 077 (2017).
- <sup>15</sup>G. Mazzitelli, V. C. Antochi, E. Baracchini, G. Cavoto, A. De Stena, E. Di Marco, M. Marafini, D. Pinci, F. Renga, S. Tomassini, and C. Voena, “A high resolution tpc based on gem optical readout,” in 2017 IEEE Nuclear Science Symposium and Medical Imaging Conference (NSS/MIC) (2017) pp. 1–4.
- <sup>16</sup>D. Pinci, E. Baracchini, G. Cavoto, E. D. Marco, M. Marafini, G. Mazzitelli, F. Renga, S. Tomassini, and C. Voena, “High resolution tpc based on optically readout gem,” Nuclear Instruments and Methods in Physics Research Section A: Accelerators, Spectrometers, Detectors and Associated Equipment (2018), <https://doi.org/10.1016/j.nima.2018.11.085>.
- <sup>17</sup><http://w3.lnf.infn.it/3d-printing-facility-lnf/>.
- <sup>18</sup>D. Pinci, *A triple-GEM detector for the muon system of the LHCb experiment*, Ph.D. thesis, Cagliari University, CERN-THESIS-2006-070 (2006) CITATION = CERN-THESIS-2006-070; .
- <sup>19</sup><http://www.hamamatsu.com/jp/en/C13440-20CU.html>.
- <sup>20</sup><http://www.hzcpotonics.com/products/XP3392.pdf>.
- <sup>21</sup>G. Mazzitelli, A. Ghigo, F. Sannibale, P. Valente, and G. Vignola, “Commissioning of the daφne beam test facility,” Nuclear Instruments and Methods in Physics Research Section A: Accelerators, Spectrometers, Detectors and Associated Equipment **515**, 524 – 542 (2003).
- <sup>22</sup>V. Kraus, M. Holik, J. Jakubek, M. Kroupa, P. Soukup, and Z. Vykydal, “FITPix — fast interface for timepix pixel detectors,” Journal of Instrumentation **6**, C01079 (2011).
- <sup>23</sup>B. Buonomo, C. Di Giulio, L.G. Foggetta, and P. Valente, “A hardware and software overview on the new btf transverse profile monitor,” in Proc. 5th Int. Beam Instrumentation Conf. (IBIC’16), Barcelona, Spain (2016) pp. 818–821.
- <sup>24</sup>P. Valente, B. Buonomo, C. Di Giulio, and L.G. Foggetta, “Frascati beam-test facility (btf) high resolution beam spot diagnostics,” in Proc. 5th Int. Beam Instrumentation Conf. (IBIC’16), Barcelona, Spain (2016) pp. 222–225.
- <sup>25</sup>R. Campagnola, *Study and optimization of the light-yield of a triple-GEM detector*, Master’s thesis, Sapienza University of Rome (2018) CERN-THESIS-2018-027 .
- <sup>26</sup>N. Torchia, *Development of a tracker based on GEM optically readout*, Master’s thesis, Sapienza University of Rome (2016) CERN-THESIS-2016-335 .
- <sup>27</sup><http://www.caen.it/csite/CaenProd.jsp?parent=21&idmod=894>.
- <sup>28</sup>G. Corradi, F. Murtas, and D. Tagnani, “A novel high-voltage system for a triple GEM detector,” Nucl. Instrum. Meth. A **572**, 96–97 (2007).
- <sup>29</sup>R. O. Duda and P. E. Hart, “Use of the hough transformation to detect lines and curves in pictures,” Commun. ACM **15**, 11–15 (1972).
- <sup>30</sup>R. Veenhof, “Garfield, a drift chamber simulation program,” Conf. Proc. C **9306149**, 66–71 (1993).
- <sup>31</sup>R. Veenhof, “GARFIELD, recent developments,” Nucl. Instrum. Meth. A **419**, 726–730 (1998).
- <sup>32</sup>I. A. Costa, E. Baracchini, F. Bellini, L. Benussi, S. Bianco, M. Caponero, G. Cavoto, G. D’Imperio, E. D. Marco, G. Maccarrone, M. Marafini, G. Mazzitelli, A. Messina, F. Petrucci, D. Piccolo, D. Pinci, F. Renga, F. Rosatelli, G. Saviano, and S. Tomassini, “Performance of optically readout GEM-based TPC with a 55Fe source,” Journal of Instrumentation **14**, P07011–P07011 (2019).
- <sup>33</sup>W. Blum, L. Rolandi, and W. Riegler, *Particle detection with drift chambers*, Particle Acceleration and Detection, ISBN = 9783540766834 (2008).
- <sup>34</sup>M. Marafini, V. Patera, D. Pinci, A. Sarti, A. Sciubba, and N. M. Torchia, “Study of the Performance of an Optically Readout Triple-GEM,” IEEE Transactions on Nuclear Science **65**, 604–608 (2018).
- <sup>35</sup>I. A. Costa, E. Baracchini, F. Bellini, L. Benussi, S. Bianco, M. Caponero, G. Cavoto, G. D’Imperio, E. D. Marco, G. Maccarrone, M. Marafini, G. Mazzitelli, A. Messina, F. Petrucci, D. Piccolo, D. Pinci, F. Renga, F. Rosatelli, G. Saviano, and S. Tomassini, “Performance of optically readout GEM-based TPC with a 55Fe source,” Journal of Instrumentation **14**, P07011–P07011 (2019).